Ozone-sensitive channel selection over IASI full spectrum with correlated observation errors for NWP

Olivier Coopmann[1], Vincent Guidard[1], Béatrice Josse[1], Virginie Marécal[1], and Nadia Fourrié[1]

[1]CNRM, Université de Toulouse, Météo-France, CNRS, Toulouse, France

Correspondence: O. Coopmann, Météo-France, CNRM/GMAP/OBS, 42 Avenue Gaspard Coriolis, 31057 Toulouse Cedex, France (olivier.coopmann@umr-cnrm.fr);V. Guidard (vincent.guidard@meteo.fr)

Abstract.

The Infrared Atmospheric Sounding Interferometer (IASI) onboard the Metop satellites provides 8461 channels in the infrared spectrum, covering the spectral interval 645 - 2760 cm^{-1} at a resolution of 0.5 cm^{-1}. The high volume of data observation resulting from IASI presents many challenges. In current Numerical Weather Prediction (NWP) models, assimilating
5   all channels is not feasible, due to data transmission, data storage and significant computational costs. One of the methods for reducing the data volume is the channel selection. Many NWP centres use a subset of 314 IASI channels including 15 ozone-sensitive channels. However, this channel selection has been carried out assuming uncorrelated observation errors. In addition, these ozone-sensitive channels have been selected only for ozone information.

The objective of this study is to carry out a new selection of IASI ozone-sensitive channels from the full spectrum over a spec-
10   tral range of 1000 - 1070 cm^{-1}, in a direct radiance assimilation framework. This selection is done with a full observation error covariance matrix to take into account cross-channel error correlations. A sensitivity method based on the channel spectral sensitivity to variables and a statistical approach based on the Degrees of Freedom for Signal (DFS) have been chosen. To be representative of atmospheric variability, 345 profiles from around the world over a one-year period were selected. The new selection, is evaluated in a One-Dimensional Variational (1D-Var) analyses framework.

15   This selection highlights a new set of 15 IASI ozone-sensitive channels. The results are very encouraging since by adding these 15 channels to 122 operational channels, temperature and humidity analyses are improved by 13.8 % and 20.9 % respectively. Obviously, these 15 channels significantly improve ozone analyses. In addition to considering inter-channel observation error correlations, the channel selection method uses a robust background error covariance matrix that takes into account temperature, humidity and ozone errors using a lagged forecast method over a one-year period. The new selection of IASI ozone-
20   sensitive channels will be soon used in the global 4D-Var ARPEGE (Action de Recherche Petite Echelle Grande Echelle) data assimilation system.

1 Introduction

The use of satellite observations in data assimilation systems has greatly advanced Numerical Weather Prediction (NWP) models. In particular, observations from infrared sounders have significantly improved the quality of weather forecasts (Hilton et al., 2012). At Météo-France, ARPEGE (Action de Recherche Petite Echelle Grande Echelle) is the global NWP model used

5 in operations (Courtier et al., 1991) and provides forecasts up to 102 h. The Four Dimensional Variational (4D-Var) data assimilation system that provides the initial conditions to ARPEGE uses 75 % of observations from infrared sounders. The major contributor is the Infrared Atmospheric Sounding Interferometer (IASI), which alone accounts for 60 % of the data assimilated in the NWP global model ARPEGE. The IASI instrument was jointly developed by CNES (Centre National d'Études Spatiales) and EUMETSAT (European Organisation for the Exploitation of Meteorological Satellites). It was first launched in 2006 on

10 board the MetOp-A polar orbiting satellite. The second instrument was launched on board MetOp-B in 2012, the last one, was launched on board MetOp-C in 2018. Its spectrum ranges from 645 to 2760 cm^{-1} with a spectral sampling of 0.25 cm^{-1} and a spectral resolution of 0.5 cm^{-1} leading to a set of 8461 radiance measurements. The high volume of data resulting from IASI presents many challenges, particularly in the areas of data transmission, data storage and information content for example. The methods for reducing the data volume are channel selection, spatial sampling or principle components analysis. A selection

15 of 300 channels was performed by (Collard, 2007) for NWP purposes. Channels were mainly selected in the CO_2 long wave (LW) band (for temperature retrievals), in the atmospheric window regions (for surface properties and clouds), in the water vapour (H_2O) band (for humidity retrievals) and in O_3 long wave band (for ozone retrievals). CNES added 14 other channels for climate monitoring purposes. Thus, this reduces the use of IASI data to 1.5 % of the full spectrum.

20 NWP models have evolved rapidly, resulting in significant improvements in the quality and accuracy of weather forecasts. However, many centres have increased their computing capability to assimilate more satellite observations. An interesting approach is the additional assimilation of observation sensitive to atmospheric composition compatible with a coupled assimilation of the Earth system. This strategy is followed by the ECMWF (European Centre for Medium-Range Weather Forecasts) leading to the use of the NWP model IFS (Integrated Forecasting System) for weather forecasting and the modelling of the

25 atmospheric composition (greenhouse gases, aerosols, and chemical species). Ozone is potentially beneficial because these sensitive channels are also sensitive to temperature and humidity and they can therefore provide additional information in 4D-Var data assimilation. Indeed, the work of (Derber and Wu, 1998) showed that a realistic ozone information improves the use of ozone-sensitive channel satellite radiances in the High Infra-red Resolution Sounder (HIRS) in the global forecast system at NCEP (National Centers for Environmental Prediction). (Semane et al., 2009) showed potential benefits of 4D-Var

30 ozone assimilation for the improvement of the wind field through dynamics-ozone coupling with the global model ARPEGE. Many more studies have shown the benefits of ozone assimilation for NWP. Since ozone is part of the control variable of the 4D-Var IFS, the assimilation of 16 IASI ozone-sensitive channels (from their own channel subset) in operation improves ozone analyses (Han and McNally, 2010), (Dragani and McNally, 2013). (Lupu and McNally, 2013) have shown the positive impact on wind analysis of assimilating ozone-sensitive channels from the Spinning Enhanced Visible and Infrared Imager (SEVIRI)

instrument on board the MSG (Meteosat Second Generation) geostationary satellite. Finally, (Coopmann et al., 2018) showed that the assimilation of 15 IASI ozone-sensitive channels from Collard's channel selection, provides additional information to improve temperature, humidity and ozone analyses. However, the 15 IASI ozone-sensitive channel selection from Collard has been carried out only for extracting ozone information with a diagonal observation-error covariance matrix ($\mathbf{R}$ in (Ide et al.,

5 1997) notation used in this paper). Indeed, since the beginning of the use of infrared observations for NWP, channel selections have been mostly performed often using diagonal $\mathbf{R}$ matrices such as those made by (Fourrié and Thépaut, 2003) for AIRS (Atmospheric Infrared Sounder) and (Gambacorta and Barnet, 2013) for CrIS (Cross-track Infrared Sounder).

This study is a preparatory work towards the use of additional IASI channels in the global 4D-Var operational system at

10 Météo-France, which assimilate IASI level 1 data. The objective is to carry out a ozone-sensitive channel ranking to obtain an additional gain on thermodynamic information (temperature, humidity) and to make a new channel selection using a full $\mathbf{R}$ matrix. To achieve this, a pre-selection using physical method based on non-linear sensitivity study and ranking selection with Degrees of Freedom for Signal (DFS) method has been undertaken. Important prerequisites for a beneficial interaction between additional IASI information and the 4D-Var system, are the use of accurate IASI observations, ozone background (or

15 *a priori*) and their respective errors. Hence, the following inputs and operator have been used:

- Ozone background profiles come from the three dimensional MOCAGE (Modèle de Chimie Atmosphérique à Grande Échelle) Chemistry Transport Model (CTM) (Guth et al., 2016) of Météo-France. This ozone field is consistent with dynamical fields of the global model ARPEGE as MOCAGE is forced by ARPEGE dynamics.

- The Radiative Transfer Model (RTM) RTTOV (Radiative Transfer for TOVS; TOVS: TIROS Operational Vertical

20 Sounder and TIROS: Television Infrared Observation Satellite) simulated IASI radiances from thermodynamic information of the global model ARPEGE.

- Realistic observation error covariance matrix from a diagnostic method including IASI interchannel correlations (Desroziers et al., 2005).

- A background error covariance matrix including ozone, temperature and humidity errors with inter-variable correlations,

25 computed with lagged forecast method.

The article is structured as follows, Section 2 presents an overview of the MOCAGE CTM, the IASI instrument, its use in the NWP ARPEGE system, and a description of the case study. We then introduce in Section 3, results of simulated IASI observations over the full spectrum and the pre-selection of all ozone-sensitive channels using a physical method based on non-linear sensitivity. The diagnosed observation error covariance matrix taking into account the IASI inter-channel error

30 correlations is computed and the background error covariance matrix including ozone is also investigated with a lagged forecast method. Section 4 describes the channel selection method to extract information content of IASI ozone-sensitive data. Then, channel selection are evaluated with 1D-Var experiments on top of the operational IASI channel dataset and the final selected ozone-sensitive channel selection for NWP are presented. Finally, Section 5 summarizes the results and opens discussion.

2   Model and data

2.1   Description of the case study

To perform a channel selection in an optimal way, IASI pixels from MetOp-A and MetOp-B have been selected and collocated around a subset of 40 radiosounding launching sites spread all over the globe (Figure 1). Temperature, humidity and ozone in-situ data were measured at different latitudes, considering several atmospheric scenarios. These profiles available from the collection of the World Ozone and Ultraviolet Data Center (WOUDC) have been selected between March 2016 and March 2017 to take into account the annual variability and have been used as verification data in Section 5.
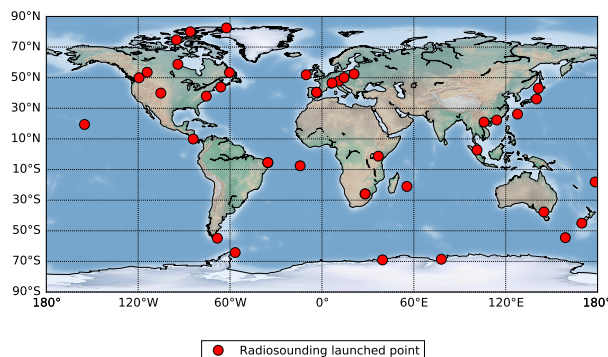
Figure 1. Map of radiosounding launched point (40 sites in red) and 345 sonde profiles from WOUDC networks.

Collocations between radiosondes and IASI pixels have been carried out using several criteria defined such as to select the closest pixel for each radiosonde. The smallest orthodromic distance with a maximal threshold of 100 km and a maximal temporal difference of 60 min between IASI pixel and radiosonde were retained. The IASI instrument also includes an Integrated Imaging Subsystem (IIS) that allows to coregister interferometric measurements with high resolution imager AVHRR (Advanced Very High Resolution Radiometer) (Saunders and Kriebel, 1988). AVHRR provides cloud and heterogeneity information in each IASI pixel. To avoid the use of cloudy pixels, IASI observations are discarded whenever the AVHRR cloud cover is above 0 %. Hence, a subset of 345 radiosondes each collocated with one IASI pixel has been selected including 222 pixels over land, 106 over sea and 17 over sea ice.

Then, the *a priori* atmospheric profiles of temperature, specific humidity, surface temperature, surface humidity, surface pressure, zonal and meridian surface winds come from the global model ARPEGE forecasts (every 3 hr), which were extracted for the same period and location as for the IASI pixels as well as ozone profiles from MOCAGE. NWP and CTM models have σ-hybrid vertical coordinates (105 levels in ARPEGE and 60 levels in MOCAGE with model top at 0.1 hPa), which were interpolated onto the 54 fixed-pressure levels of the RTM RTTOV model. In order to use a realistic surface temperature, the skin temperature is retrieved from the radiative transfer equation inversion using IASI window channel 1194 (943.25 cm^{-1})

((Boukachaba, 2017) and (Vincensini, 2013)) for each pixel. This retrieval relies on the specification of emissivity values over land from The Combined ASTER MODIS Emissivity over Land (CAMEL) (Borbas et al., 2018) and from a surface emissivity model (ISEM) (Sherlock and Saunders, 1999) over the open sea and sea ice. Thus, in the following, we will not assimilate this particular IASI window channel.

2.2 MOCAGE model

MOCAGE is an off-line global three-dimensional chemistry transport model (Josse et al., 2004), (Guth et al., 2016). It provides the time evolution of the chemical air composition from the surface to the stratosphere. This model is used for operational daily forecasts e.g. (Marécal et al., 2015) and also for research studies e.g. (Bousserez et al., 2007), (Anderson et al., 2017), (Morgenstern et al., 2017), (Guth et al., 2018).

The meteorological fields (temperature, wind, specific humidity, pressure, cloud and precipitation) used here in MOCAGE come from outputs of a separate meteorological model, ARPEGE. The advection of chemical species in MOCAGE follows the semi-lagrangian approach of (Williamson and Rasch, 1989). Sub-grid scale convection and diffusion are represented using (Bechtold et al., 2001) and (Louis, 1979), respectively. Dry deposition comes from (Wesely, 2007) parametrisation. Scavenging of trace gases by stratiform and convective precipitation follows (Giorgi and Chameides, 1986) and (Mari et al., 2000), respectively. Gas chemistry is based on RACM (Regional Atmospheric Chemistry Mechanism) chemical scheme (Stockwell et al., 1997) for the troposphere, and REPROBUS (Reactive Processes Ruling the Ozone Budget in the Stratosphere) (Lefevre et al., 1994), (Lefèvre et al., 1998) for the stratosphere. This leads to a total of 115 gas species and 372 reactions.

Ozone from MOCAGE simulations was already used by (Coopmann et al., 2018) in their 1D-Var data assimilation of IASI ozone-sensitive channels. Since then, MOCAGE chemistry was improved. All thermal reaction rates were updated following the latest version of JPL (Jet Propulsion Laboratory) recommendations (Burkholder et al., 2015). Photolysis rates are calculated in MOCAGE via a look-up table computed off-line. This table was updated using TUV (The Tropospheric Ultraviolet and Visible) software version 4.6 (Madronich, 1987). Also the photolysis of PAN (Peroxyacetic Nitric Anhydride) was added. All these changes provide improvements to ozone in MOCAGE, particularly in the Upper Troposphere and Lower Stratosphere (UTLS) where ozone plays an important role on the radiation. Ozone profiles from MOCAGE are used in this study for two purposes: firstly, as input to the RTM for the simulation of IASI radiances, and secondly, to calculate the background error covariance matrix with a lagged forecast approach.

2.3 Radiative Transfer Model

To extract information from IASI radiances, we need to confront them with what the model already knows. For this purpose, IASI observations are simulated with a RTM known as RTTOV. RTTOV simulates the top of the atmosphere clear-sky radiances in the visible, infrared and microwave spectrum. In the data assimilation formalism, differences between observations and simulated counterparts formulated as $\mathbf{d}_b^o = \mathbf{y}^o - \mathcal{H}(\mathbf{x}^b)$ are known as First Guess (FG) departure or innovation, where $\mathbf{y}^o$ is the

observation, $\mathbf{x}^b$ is the background and $\mathcal{H}$ is the observation operator, which simulates radiances from $\mathbf{x}^b$ through the RTM. To accurately simulate satellite observations, RTTOV requires knowledge of thermodynamic and chemical profiles that represent the most probable atmospheric state at the time of the measurement by the satellite instrument.

2.4 IASI satellite data
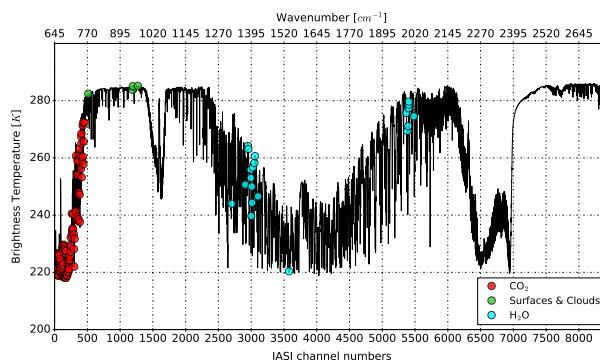
Figure 2. The IASI infrared spectrum in Brightness Temperature simulated for a standard mid-latitude clear sky profile (black) and 123 IASI channels operationally assimilated at Météo-France; 99 CO_2 sensitive channels (red), 4 window channels (green) and 20 H_2O sensitive channels (cyan).

5   IASI is a Michelson interferometer measuring 8.461 spectral samples between 3.62 and 15.5 μm with a resolution of 0.5 cm^{-1} after apodisation. IASI scans cross-track in 30 successive elementary fields of view (EFOV), each composed of 4 instantaneous fields of view (IFOV). The EFOV's span a $\pm48.33°$ range, symmetric with respect to the Nadir, in steps of 3.33°. The swath width on the ground is approximately 2,200 km, which provides global Earth coverage twice a day. The IFOV is a disc or pixel of 12 km diameter at sub-satellite point (August et al., 2012). The shape of the IFOV at the edge of the scan

10 line is an ellipse: across track, it measures 39 km and along track, 20 km. This sounder provides indirect information on temperature and humidity profiles to be obtained along with that of cloud cover, aerosols, atmospheric chemistry compounds such as O_3, CO_2, CO, CH_4, HNO_3 and N_2O (Clerbaux et al., 2009) and surface properties. The IASI mission accuracy requirement is 1 K for tropospheric temperature and 10 % for humidity for a vertical resolution of 1 km (Hilton et al., 2012).

15   A subset of 314 channels corresponding to Collard's selection is routinely monitored at Météo-France and up to 123 channels are assimilated in operations; 99 temperature channels in the LW CO_2 band [650 to 770 cm^{-1}], 4 window channels [790 to 980 cm^{-1}] and 20 H_2O channels [1210 to 1650 cm^{-1}] (Figure 2). The sensitivity of this subset to temperature, humidity, ozone and skin temperature is evaluated by computing their mean Jacobians for 345 *a priori* profiles (Figure 3). The Jacobian represents the sensitivity of the Brightness Temperature (BT) with respect to a change in thermodynamic or chemical parame-

20 ters. Jacobians for temperature (T), humidity (q), ozone (O_3) and skin temperature (T_{skin}) were calculated with RTM RTTOV. Jacobians of humidity and ozone were multiplied by 10 % of their concentrations to overcome the large variability of these
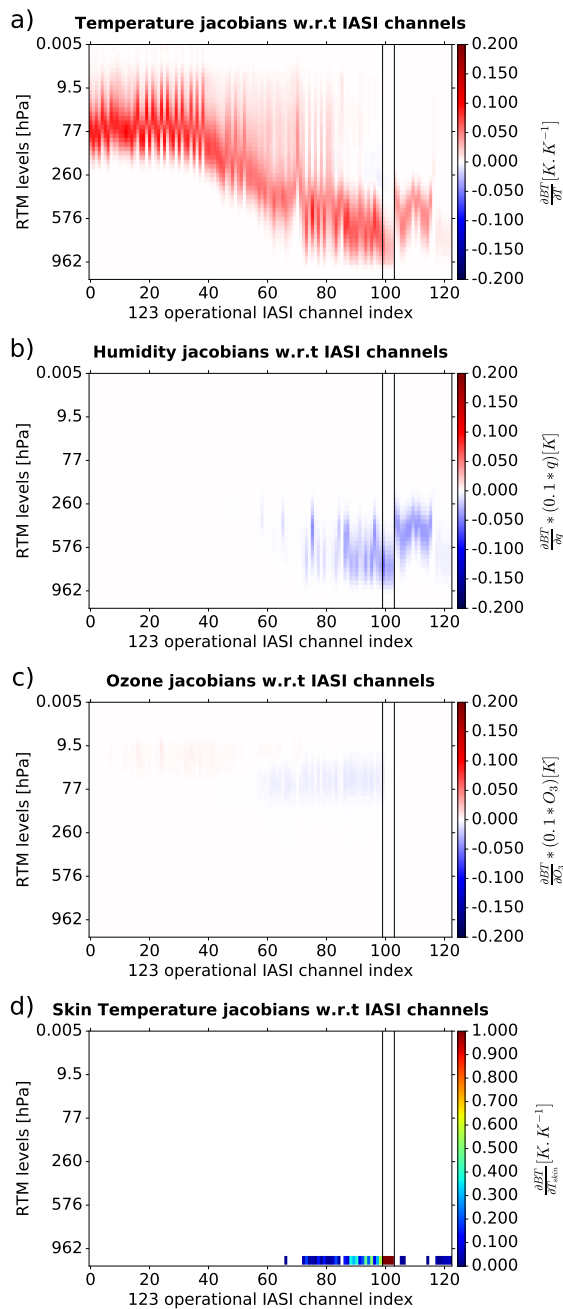
Figure 3. Mean Jacobians of temperature (a), humidity (b), ozone (c) and skin temperature (d) for 123 IASI operational channels at Météo-France w.r.t. 54 RTM pressure levels [hPa].

parameters.

Temperature Jacobians (Figure 3.a) for the 99 CO_2 sensitive channels **[index 0 to 99]** show sensitivity from the lower troposphere up to the top of the stratosphere with a higher value in the stratosphere with a maximum around 0.10 K K^{-1}. The 4 window channels **[index 100 to 103]** show very low sensitivity to atmospheric temperature. The 20 H_2O sensitive channels **[index 104 to 123]** show high sensitivity in the troposphere with a maximum value around 0.15 K K^{-1}. All the channels

5 have temperature-sensitive Jacobians because by definition the radiative transfer equation involves this parameter. Humidity Jacobians (Figure 3.b) for the CO_2 sensitive channels show no sensitivity except for 72 to 99 channel indices with values around 0.05 K. Window channels show some sensitivity in lower troposphere. The H_2O sensitive channels exhibit higher values in the mid-troposphere for the 103 to 115 channel index with a maximum around 0.12 K and lower values for the 116 to 123 channel index. Ozone Jacobians (Figure 3.c) show almost no sensitivity. Finally, skin temperature Jacobians (Figure 3.d) show

10 low sensitivity for the channels on each side of the atmospheric window with values between 0.10 to 0.40 K K^{-1}. Window channels show higher values around 0.90 K K^{-1}. Overall, we notice that the 123 channels are almost insensitive to ozone. They provide temperature sensitivity over a large part of the atmosphere. Water vapour sensitive channels have Jacobians of humidity whose values are high on mid tropospheric where there is on average the most humidity.

3 Experimental framework

15 ### 3.1 Simulated IASI observations
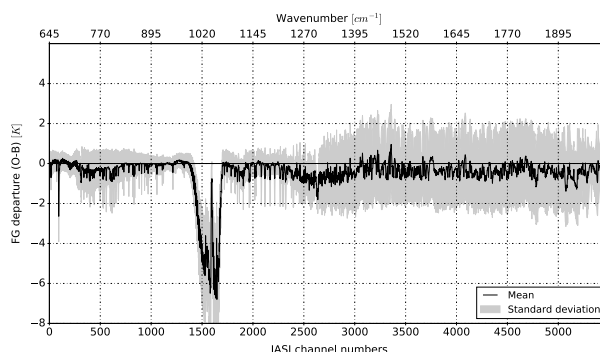
Figure 4. Mean and standard deviation of FG departures with respect to 5500 IASI channels number and wavenumber (IASI bands 1 & 2) using a set of 345 profiles.

In this experiment, we simulated the IASI radiances for the 345 pixels collocated with the 345 radiosondes using in RT-TOV the 345 profiles *a priori* from the ARPEGE model. The simulations for the 345 case studies were compared with real IASI observations and statistics calculated (in Brightness Temperature) on the channels contained in spectral bands 1 and 2 (5500 channels). Mean and standard deviation of FG departures show different values according to spectral range (Figure 4).

20 Generally, mean FG departures display values less than 0.75 K with standard deviation between 0.25 to 2.00 K, except for O_3 sensitive channels. Indeed, we note a large mean of FG departures between 1000 to 1070 cm^{-1} with values up to 7.00 K

and standard deviation between 0.50 to 2.50 K. The ozone profiles from MOCAGE are realistic but do not represent reality, hence the important bias of ozone-sensitive channels. However, the study conducted by (Coopmann et al., 2018) showed that the standard deviation of FG departures are 3 times lower for IASI ozone-sensitive channels using realistic ozone profiles from MOCAGE than the reference ozone profile available in RTTOV. The mean of FG departures calculated in this experiment is

5   used to perform a static bias correction of IASI observations for the next step.

3.2 Pre-selection of O_3 channels based on a physical method

First step of channel selection is the identification of IASI ozone-sensitive channels over the full spectrum. For this purpose, we have used the methodology developed by (Gambacorta and Barnet, 2013) for the Cross-track Infrared Sounder (CrIS) instrument. This method involves assessing sensitivity of the brightness temperature response ΔBT, represented by the difference

10   between RTTOV simulations with unperturbed and perturbed profiles. Only the vertical ozone profile was modified with a constant perturbation, typically 10 % for the perturbed simulations. Same background datasets from previous simulation experiments were used. The ΔBT indicates the sensitivity of each channel to ozone in all atmospheric cases (345).

The largest ΔBT sensitivity of IASI channels is located between 645 - 770 cm^{-1} and 970 - 1095 cm^{-1}, with values around

15   0.20 and 1.25 K (Figure 5.a). Sensitivity identified between 645 - 770 cm^{-1} is for CO_2 sensitive channels already used operationally to extract temperature content. Only IASI channels between 970 - 1095 cm^{-1} and above the instrumental noise have been pre-selected. Thus, a sample of 306 IASI ozone-sensitive channels has been retained. These channels are shown in Figure 5.b.

20   We examine the Jacobians of 306 pre-selected ozone-sensitive channels w.r.t temperature, humidity, ozone and skin temperature in Figure 6 as it has been done for operational IASI channels (Figure 3). Temperature Jacobians (Figure 6.a) **[index 0 to 306]** show sensitivity in the lower troposphere up to the mid-troposphere with a maximum value of around 0.05 K K^{-1} due to the high concentration of tropospheric ozone. The rather sensitive channels in the stratosphere have high Jacobian temperature values towards the mid-stratosphere where stratospheric ozone concentrations are highest. Figure 6.b reveals a humidity sensi-

25   tivity in the lower troposphere with a maximum value of around 0.05 K. Ozone Jacobians (Figure 6.c) have high sensitivity in the middle of the stratosphere with maximum values around 0.15 K corresponding to the region of the atmosphere having the largest stratospheric ozone concentrations. Finally, skin temperature Jacobians (Figure 6.d) show a large sensitivity between [0 to 75], [190 to 210] and [295 to 306] channel index with values between 0.70 to 1.0 K K^{-1}. Indeed, the channels with high values of skin temperature Jacobians are channels close to atmospheric windows. These Jacobians of the 306 pre-selected O_3

30   channels indicate a potential of additional information on temperature, humidity and skin temperature compared to operational IASI channels especially for temperature and humidity in lower troposphere.
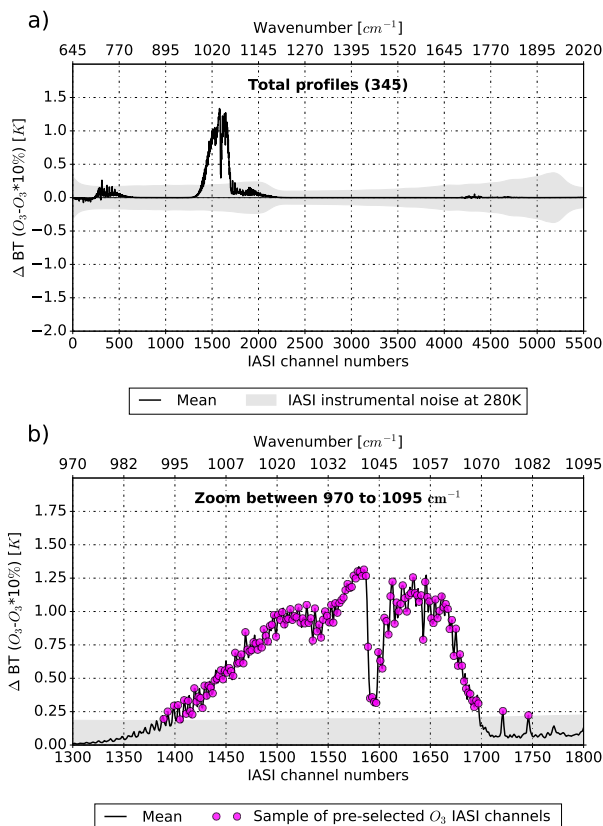
Figure 5. Mean of differences between simulations with the unperturbed and perturbed ozone profiles (ΔBT) w.r.t. IASI channels and wavenumbers [cm^{-1}] using a set of 345 profiles (a). Sample of pre-selected ozone-sensitive channels between 970 and 1095 cm^{-1} for ΔBT using total datasets (b). The shaded area represents IASI instrumental noise at 280 K.

3.3 Background errors

The National Meteorological Centers (NMC) method by (Parrish and Derber, 1992) is a technique that defines background errors from the difference between NWP forecasts of various range valid at the same time. This method is here apllied to ozone forecasts. We consider differences from between 36 h and 12 h forecast ranges. The background error covariance matrix (**B** in (Ide et al., 1997) notation used in this paper) is then constructed using long-term modelling results. MOCAGE was run to provide temperature, specific humidity (from ARPEGE) and ozone 3D distributions. Two twin simulations were performed. For each one, the configuration uses 60 hybrid levels, from the ground up to 0.1 hPa, and a global domain with a 1 ° horizontal resolution. The model was run from September 2016 to April 2018, the first 6 months being considered as spin-up. Meteorological inputs from ARPEGE to MOCAGE given every 3 h. Simulation method is illustrated in Figure 7:

©c Author(s) 2019. CC BY 4.0 License.
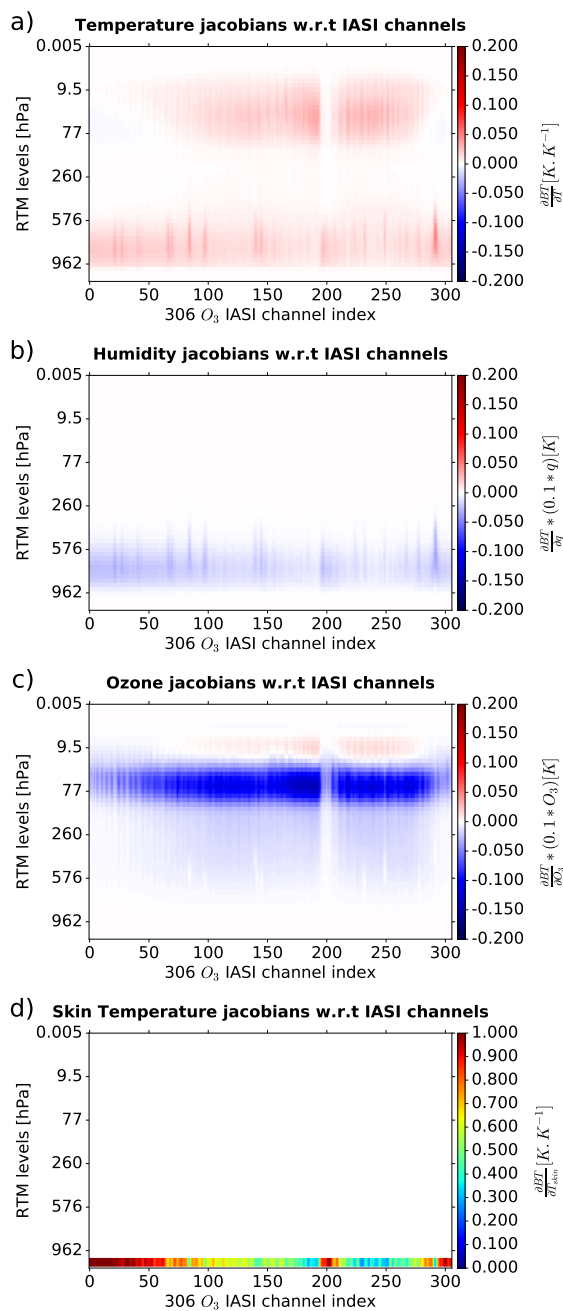
Figure 6. Jacobians in temperature (a), humidity (b), ozone (c) and skin temperature (d) for 306 O_3 IASI channels pre-selected w.r.t. 54 RTM pressure levels [hPa].

- In the first simulation (MOC+12H), every day an ozone forecast up to 24 h range is produced using ARPEGE forecasts starting from an analysis at 00 UTC. The chemical fields for the day D at 24 h are used as the initial chemical fields of the day D+1 at 00 h. 1.5 yr simulation has been produced with this cycling mode;

- In the second simulation (MOC+36H), an ozone forecast up to 36 h range is produced using MOC+12H ozone initial field and using 36 h range meteorological fields from the ARPEGE forecast starting at D, 00 UTC.

Finally, **B** matrix is computed statistically from MOC+12H/MOC+36H forecast differences, valid at the same time, over a
5   one year period (March 2017 to March 2018). The MOCAGE fields were interpolated on the 54 RTM pressure levels before computing statistics.
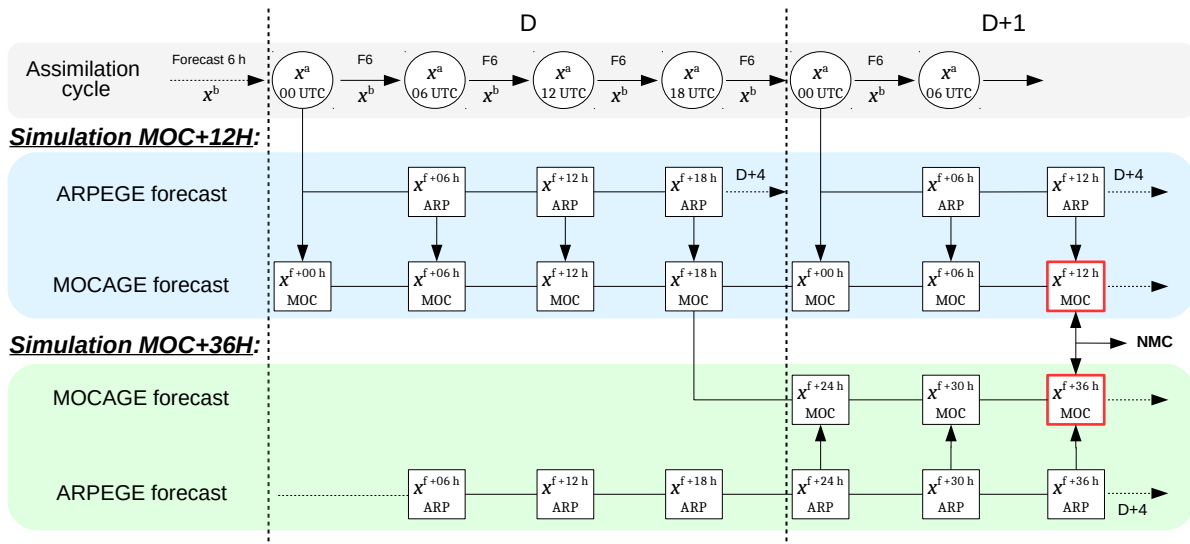
Figure 7. Schematic illustration of the NMC method using ARPEGE and MOCAGE models, where x_{MOC}^{f+12h}. is the forecast from simulation MOC+12H that valid at time D ; Similarly, x_{MOC}^{f+36h} is the forecast from simulation MOC+36H that valid at time D+1.

Figure 8 shows the background error standard deviation (σ) of temperature (a), logarithm of specific humidity (b) and ozone (c) with respect to pressure. We observe values of σ_T^b around 0.5 and 1.5 K between 1000 and 10 hPa, then values increase up
10   to 3.0 K at 0.1 hPa. We note a peak of $\sigma_{log(q)}^b$ values around 0.6 log(kg/kg) beween 600 and 400 hPa. Then, $\sigma_{O_3}^b$ values show two peaks around 0.65 ppmv at 25 and 2 hPa. Finally, Figure 8 shows the background error correlation matrix of temperature (d), humidity (e) and ozone (f) with respect to model levels. Significant positives correlation are observed for temperature in the troposphere and upper stratosphere. We also note negative correlations in the UTLS. Then, the same trends are noticed for the humidity correlation in troposphere. Correlations of ozone are noticed for all atmospheric levels. The high positive correlations
15   in temperature, humidity and ozone at the top of the stratosphere are caused by field interpolation to be set on RTM pressure levels. Indeed, RTM pressure levels rise to 0.005 hPa while MOCAGE pressure levels rise only to 0.1 hPa. These results are consistent with the work carried out by (Berre, 2000) and (Hólm and Kral, 2012).

This **B** matrix will be used for the channel selection. In this study, a univariate **B** matrix is chosen, which means that cross-correlation between temperature, humidity and ozone variables are not taken into account. This assumption prevents feedback effects of ozone on temperature and humidity (Dethof and Holm, 2004). In addition, levels used for the background-error covariance in channel selection and 1D-Var experiments are: 49 levels for temperature between 1013 and 0.06 hPa, 27 levels

5   for humidity between 1013 and 115 hPa (no level in the stratosphere) and 49 levels for ozone between 1013 and 0.06 hPa.
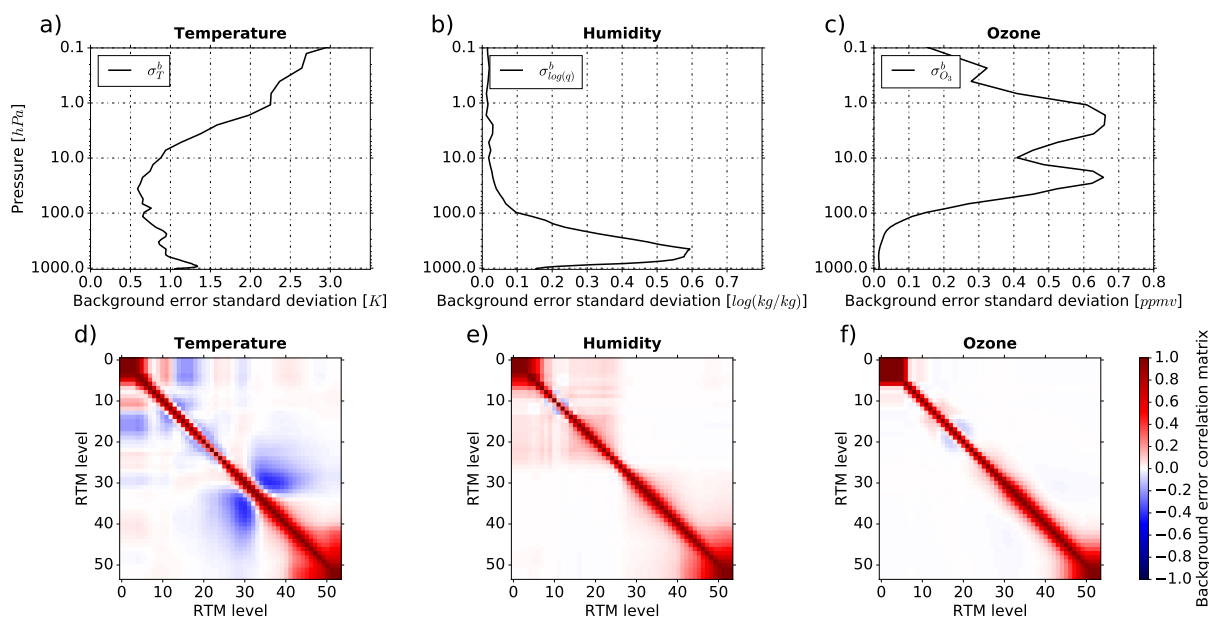
Figure 8. Standard deviation of temperature [K] (a), humidity [log(kg/kg)] (b) and ozone [ppmv] (c) background error with respect to pressure [hPa]. Background error correlation matrix of temperature (d), humidity (e) and ozone (f) with respect to RTM level. Note that level 0 is the top RTM level at 0.005 hPa and level 54 is lowest RTM level at 1050 hPa.

3.4   Correlated observation errors

Diagonal observation-error covariance matrices are convenient to specify but it has been shown that for hyperspectral infra-red sounders such hypothesis is not valid (Bormann et al., 2011). Nevertheless, few channel selection studies have used a complete observational error covariance matrix taking into account cross-channel correlations. It is worth mentioning that (Ventress and

10   Dudhia, 2014) performed a selection of IASI channels with a full **R** matrix, but like in Collard's study, the ozone-sensitive IASI channels were selected for the sole purpose of improving ozone analyses. A first step towards the estimation of realistic observation-error standard deviation is to use standard deviation derived from FG departures previously computed. This provides simulated observation-error standard deviation represented by the red line in Figure 9.a with respect to IASI channel numbers (122 operational + 306 O_3 channels). This is a useful first approach but these observation-error standard deviations

do not take into account the cross-correlation between channels.
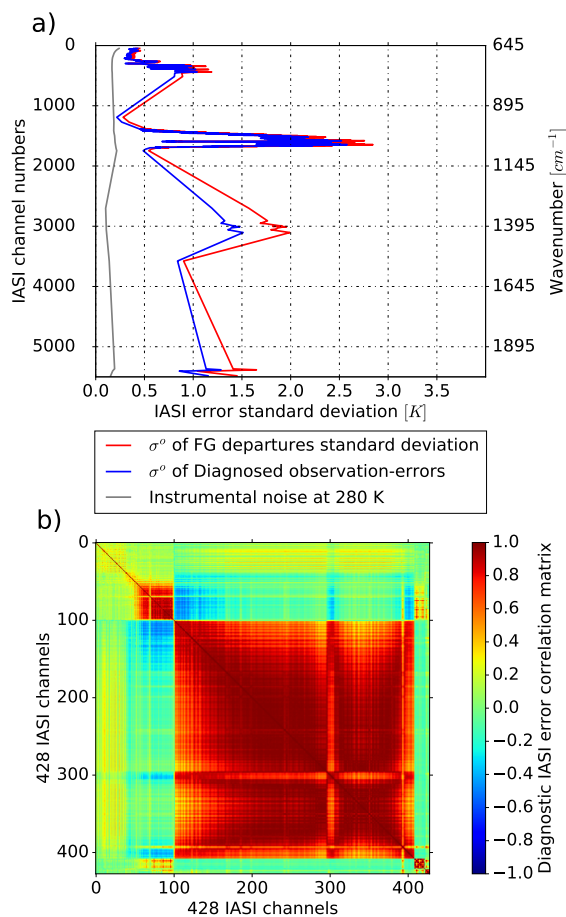
Figure 9. Simulated observation-error standard deviation with respect to IASI channel (122 operational + 306 O$_3$ channels) in red line, diagnosed observation-error standard deviation with respect to IASI channel in blue line and instrumental noise at 280 K in grey line (a). Diagnostic IASI error correlation matrix with respect to 428 IASI channels (b)

.

In order to estimate the observation-error standard deviation and more generally the structure of the observation error co-variance matrix $\mathbf{R}$, a diagnostic method introduced by (Desroziers et al., 2005) was used. Background and observation error covariance matrices can be estimated from observation departures to background and analysis. These diagnosed matrices allow to investigate if of the "*a priori*" prescribed matrices, before analysis, are correctly specified. Taking the expected value of the cross-product of $\mathbf{d}_a^o$, where the vector of analysis residuals $\mathbf{d}_a^o$ is the difference between observations $\mathbf{y}$ and the analysis state projected onto the observation space $\mathcal{H}(\mathbf{x}^a)$ such as $\mathbf{d}_a^o = \mathbf{y} - \mathcal{H}(\mathbf{x}^a)$, and using the assumption of uncorrelated errors, (Desroziers et al., 2005) found a statistical approximation for the observation error covariance matrix $\widetilde{\mathbf{R}}$ as mean diagnosed

matrix after iterations which reads: $\widetilde{\mathbf{R}} = \mathbf{E}\left[\mathbf{d}_a^o(\mathbf{d}_b^o)^\mathrm{T}\right]$, where E is the mathematical expectation. A set of 1D-Var experiments was carried out to diagnosed $\mathbf{R}$ matrix up to the convergence. This diagnostic was conducted using as a starting point a diagonal $\mathbf{R}$ matrix with variances from the standard deviations of FG departures previously calculated for the operational channels and the 306 ozone-sensitive channels. The $\mathbf{B}$ matrix calculated using the NMC method was also used. Finally, the 1D-Var

5 were made for the 345 profiles. Desroziers diagnostic is commonly used by the assimilation community, (eg at the MetOffice (Weston et al., 2014), or at ECMWF (Bormann et al., 2011)). $\widetilde{\mathbf{R}}$ includes both the instrumental errors, the observation operator errors and representativeness errors. The observation operator errors includes errors from the radiative transfer model and from the spectroscopic uncertainties. The errors of representativeness are caused when there is a scale mismatch between the model and the observation. The diagnosed observation-error standard deviations are represented by blue line with respect to

10 IASI channel numbers in Figure 9.a. The grey line represents values of instrumental noise at 280 K. We note that the values of diagnosed observation-error standard deviation for CO_2 and O_3 sensitive channels are close to simulated observation-error standard deviation while the values of diagnosed observation-error standard deviation for surface and H_2O sensitive channels are smaller than values of simulated observation-error standard deviation.

15   Figure 9.b displays the diagnosed IASI error correlation matrix from diagnosed $\widetilde{\mathbf{R}}$ matrix with respect to 428 channels. Correlation between 0 and 99 IASI channels index indicates sensitivity of CO_2 from the top of the stratosphere to the lower of the troposphere. Correlations of window channel observation errors are represented between 100 and 102 IASI channel indexes. Then, the higher correlated block between 103 and 408 IASI channel numbers represents ozone-sensitive channels. Finally, IASI channel indexes between 409 and 428 represent water vapour correlations. We note large positive correlations

20 between O_3 and stratospheric CO_2 sensitive channels while we observe negative correlation between O_3 and tropospheric CO_2 sensitive channels. Large positive correlations between tropospheric CO_2 and water vapour sensitive channels are noticed.

4   Channel selection

4.1   Ranking selection of O_3 channels based on DFS method

In the following section, the Degree of Freedom for Signal (DFS) method is used to select a set of optimal channels having

25 the largest information content for each atmospheric profile as described by (Rodgers, 2000). The DFS is based on information theory and provides a measure of the gain in information gathered by the observations according to the formula: $\text{DFS} = \text{Tr}(\mathbf{I} - \mathbf{A}\mathbf{B}^{-1})$, where Tr denotes the trace, $\mathbf{I}$ the identity matrix and $\mathbf{A}$ is the analysis-error covariance matrix with $\mathbf{A} = (\mathbf{B}^{-1} + \mathbf{H}^T\widetilde{\mathbf{R}}^{-1}\mathbf{H})^{-1}$, where $\mathbf{H}$ represent Jacobians matrix of the RTM for all channels. The background-error covariance matrix is derived from the one previously computed with the NMC method. The diagnosed $\widetilde{\mathbf{R}}$ matrix estimated for the

30 123 operational and 306 ozone-sensitive channels has been used.

The DFS_{TOT} has been chosen as a figure of merit, where DFS_{TOT} is the sum of temperature DFS_T, humidity DFS_q, ozone $\text{DFS}_{\mathrm{O}_3}$ and skin temperature $\text{DFS}_{\mathrm{T_{skin}}}$. Indeed, the consideration of each variable in the selection is important because we use
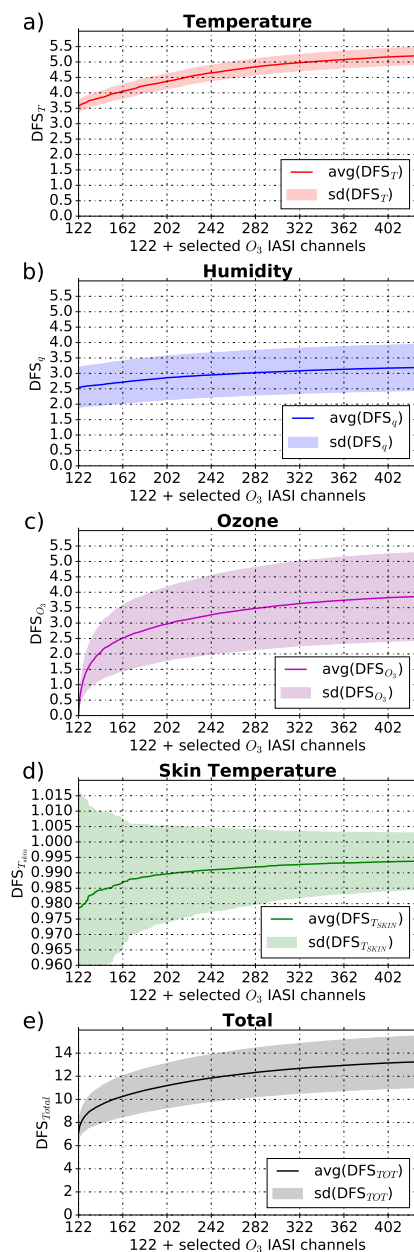
Figure 10. Evolution of the DFS statistics during the IASI O_3 channel ranking starting from the total DFS of 122 operational channels at Météo-France. The average over 345 profiles (solid line) and +/- standard deviation (coloured area) of DFS_T is represented in red (a), DFS_q is represented in blue (b), DFS_{O_3} is represented in purple (c), $DFS_{T_{skin}}$ is represented in green (d) and DFS_{TOT} is represented in black (e).

a full **R** matrix where the sensitivity of each channel is correlated with the sensitivity of the other channels. Our starting point is the mean of DFS_{TOT} value over all 345 profiles for the 122 operational channels. Then we compute all 306 combinations

of 122 channels + 1 additional O_3 channel. We select the channel providing the maximum increase in the mean of DFS_{TOT} value. The iterative process continues with 305 combinations of 123 + 1 channels and soon until all channels are selected. This means that we iteratively selected ozone-sensitive channels having the largest mean of DFS_{TOT} value on top of the DFS from the operational channels over all atmospheric profiles.

Figure 10 represents the evolution of DFS statistics (average and standard deviation over 345 profiles) during the IASI O_3 channel ranking starting from the DFS of the 122 operational channels. The evolution of the averaged DFS_T during the selection process (Figure 10.a), ranges from 3.5 for the 122 operational channels to 5.20 when using 306 additional channels. Figure 10.b shows the evolution of the averaged DFS_q which values vary from 2.54 to 3.18. Figure 10.c shows the evolution of the averaged

10 DFS_{O_3}: as expected the value is very small for the 122 operational channels (0.05) and reaches 3.86 with 428 channels. The evolution of the averaged $DFS_{T_{skin}}$ exhibits only very small variations, from 0.979 to 0.994 (Figure 10.d). Finally, the evolution of the averaged DFS_{TOT} during the selection process increase from 7.15 to 13.24 (Figure 10.e). It can be seen that overall mean of DFS values increase rapidly with the addition of 120 channels and then the lines converge towards a threshold as new ozone-sensitive channels are added. The information potential contained in these channels is therefore quickly achieved. The

15 additional gain in DFS_{TOT} is: 6.09 DFS_{TOT} = 3.80 DFS_{O_3} + 1.63 DFS_T + 0.64 DFS_q + 0.015 $DFS_{T_{skin}}$. The highest contribution comes from DFS_{O_3}. However, we note potential information from ozone-sensitive channels on temperature and humidity.

4.2 Choice of selection

The DFS method has allows to rank the most informative ozone-sensitive channels in terms of ozone, temperature, humidity and skin temperature. In order to identify the channels having the largest impact on thermodynamic analyses, we carried out

20 retrieval experiments in a one-dimensional framework (1D-Var). To identify different channel selection samples, we calculated the normalized percentage of additional total DFS, 0 % representing the total DFS for the 122 operational channels and 100 % for the 428 channels. We selected the channels for every 10 % change, summarized in Table 1. Results from 1D-Var experiments assimilating the different channel selections are compared to the results from 1D-Var experiments using the 15 ozone-sensitive channels selected by Collard.

In our assimilation experiments, the selected ozone-sensitive channels are added to the operational selection to assess the potential for providing additional information. To evaluate improvement on temperature, humidity and ozone analyses between experiments, the sum of relative error reduction (RED) of analysis profiles ($\mathbf{x}^a$) is compared to background profiles ($\mathbf{x}^b$) with respect to sondes profiles ($\mathbf{x}^s$) for all 345 profiles according to the formula:

30 $$RED = \sum_{i}^{n} \left[\frac{sd(\mathbf{x}_i^a - \mathbf{x}_i^s) - sd(\mathbf{x}_i^b - \mathbf{x}_i^s)}{sd(\mathbf{x}_i^b - \mathbf{x}_i^s)} \right] \qquad (1)$$

where (sd) defined standard deviation at each vertical level (i); n being the number of levels on which we minimize and for which there are sonde data (n=40 for temperature, n=27 for humidity and n=40 for ozone). Thus, a negative RED indicates that the analysis is closer to the sonde than the background profiles. As the sonde profiles have very high vertical resolution, we take

Normalized percentage of additional available DFS$_{TOT}$	Number of IASI O_3 channels selected
10%	2
20%	5
30%	11
34%	15
40%	22
50%	39
60%	62
70%	94
80%	135
90%	195
100%	306

Table 1. Table of number of IASI ozone-sensitive channels selected w.r.t normalized percentage of additional available DFS$_{TOT}$.

into account the IASI Averaging Kernel matrix **AK** in our RED evaluation to smooth the temperature, humidity and ozone sonde ($\mathbf{x}^{sk}$) and analysis ($\mathbf{x}^{ak}$) profiles towards the resolution of the satellite data such as: $\mathbf{x}^{ak\ or\ sk} = \mathbf{x}^b + \mathbf{AK}(\mathbf{x}^{a\ or\ s} - \mathbf{x}^b)$. In our case, the Averaging Kernels are a representation of the sensitivity of the IASI observations to changes in the atmosphere [Rodgers (2000) and Rodgers and Connor (2003)]. The Averaging Kernel matrix is calculated as follow: $\mathbf{AK} = (\mathbf{B}^{-1} + \mathbf{H}^T \widetilde{\mathbf{R}}^{-1} \mathbf{H})^{-1} \mathbf{H}^T \widetilde{\mathbf{R}}^{-1} \mathbf{H}$.

5   This method is used in many studies such as Delcloo et al. (2011) and Boylan et al. (2015).
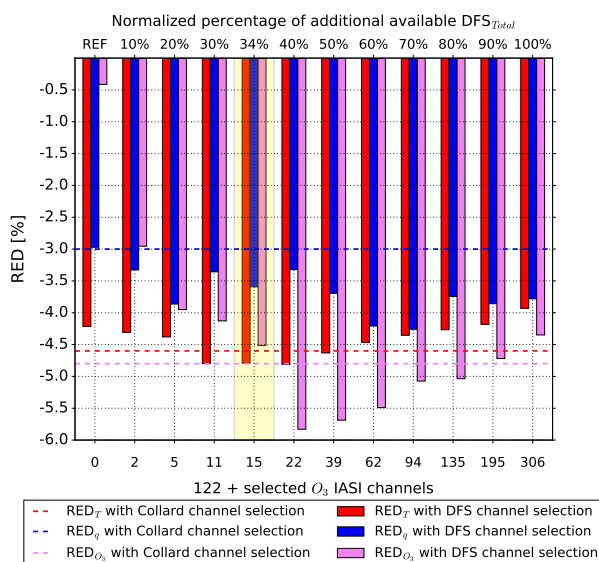
Figure 11. Evolution of the relative error reduction (RED) for temperature (red line), humidity (blue line) and ozone (purple line) using different ozone-sensitive channels selection. Dashed line for the same variables indicates the RED using Collard's channel selection.

To evaluate the impact of different O_3 channel selections on temperature, humidity and ozone analyses, the evolution of the relative error reduction for temperature (red line), humidity (blue line) and ozone (purple line) is shown in Figure 11. It appears that the RED does not evolve linearly with the addition of ozone-sensitive channels. The RED in ozone decreases very quickly with the 2 first additional channels, from -0.41 to -3.0 %. Then the RED in ozone continues to decrease until 22

5 additional channels are added with a value of -5.8 %. Finally, the use of additional channel above 22 the quality of RED in ozone up to -4.3 % when all channels are considered. For temperature, there is also an improvement in RED up to 22 channels. Then selections with more channels reduce the quality of RED until all ozone channels are added. For humidity, there are oscillations in RED on the first channel selection and then an improvement is obtained until 94 channels are added. Finally, the RED decreases slightly until all ozone-sensitive channels are added.

The non-monotonic evolution of each error reduction appears surprising at a first glance. Several factors could explain such a behaviour. Firstly, while adding more and more channels in the 1D-VAR, more minimization steps are needed. This has been accounted for by increasing the number of possible iterations. Nevertheless, it still can be difficult to disentangle the information contained in the innovations to obtain the optimal increments to the temperature, humidity and ozone profiles. Indeed,

15 even if the error covariance matrices are evaluated thanks to advanced techniques, some inconsistencies between $\mathbf{B}$ and $\widetilde{\mathbf{R}}$ still are possible. Secondly, the bias correction has been calculated over the 345 cases of the study and may not be fully optimal. This can eventually lead to some inconsistencies between the information contained in the innovations of various channels. Finally, background profiles already are of good quality (around 0.6 K between 7 and 700 hPa) and sondes are not the true state of the atmosphere.
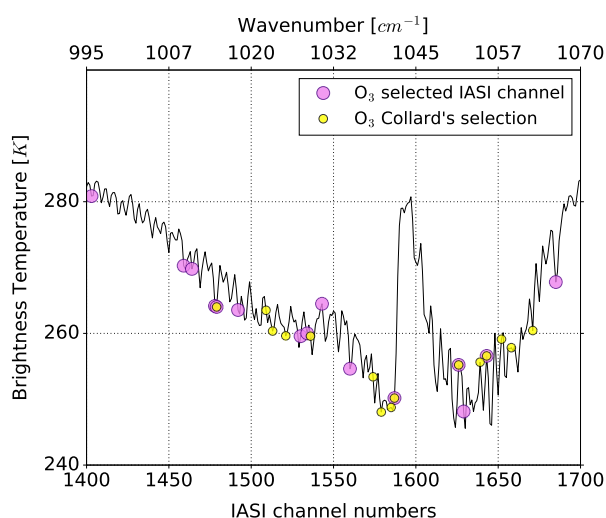
Figure 12. The IASI infrared spectrum in Brightness Temperature computed from a standard mid-latitude profile with 15 IASI ozone-sensitive channels selected (purple circles) and 15 IASI ozone-sensitive from Collard's selection (yellow circles).

It should be noted that the experiment assimilating the 15 ozone-sensitive channels selected by Collard does not reduce the RED in temperature and humidity as much as the selection of 15 ozone-sensitive channels performed in this study (dashed lines versus bars for 137 channels). However, as expected, Collard's selection allows to reduce the RED in ozone even further than our selection since it was made exclusively to improve ozone analyses. Conversely, the objective of our study is to select

5   ozone-sensitive channels with information to also improve temperature and humidity analyses. In this context, the channel selection that seems to be the best compromise to reduce temperature and humidity errors is the 15 first selected channels (representing around one third of the total DFS gain). These channels, along with those of Collard are represented in Figure 12 with a IASI infrared spectrum in BT computed from a standard mid-latitude profile. It can be seen that the channels of this selection are rather well distributed over the ozone sensitive part of the spectrum. Note that for this selection, 4 channels are

10   common with Collard's selection (1479, 1587, 1626 and 1643).

4.3   Further assessment of a 15 O_3 channel selection

In order to assess the contribution of 15 new ozone-sensitive IASI channels, we compared the vertical profiles of analysis errors and DFS from 1D-Var experiments using the 122 operational channels and 122 + 15 selected channels. We observe in Figure

15   13, that the 122 operational channels assimilation reduce the analysis error of temperature (σ^a_{122}) compared to background error especially in the troposphere between 1000 and 100 hPa and in the upper stratosphere between 10 and 0.1 hPa. Adding the 15 selected channels slightly reduces the analysis error (σ^a_{137}) compared to σ^a_{122} at the same atmospheric levels. Similarly, the 122 channels reduce analysis error of humidity especially between 900 and 150 hPa. The addition of the 15 selected channels further reduce even through very slightly the analysis error of humidity on the same part of the atmosphere. As expected, the

20   122 operational channels do not reduce the analysis error of ozone compared to the background error. The addition of the 15 selected channels reduces the ozone analysis error, especially between 1000 to 200 hPa and 100 to 15 hPa. It can be seen that the error reduction levels correspond to the levels of maximum DFS values.

Figure 14 identifies the atmospheric levels for which 1D-Var experiments (122 or 137) improve the analysis compared to

25   the background using the sonde as verification data. In Figure 14.a the vertical RED profiles for temperature for RED_{122} (black line) or RED_{137} (blue line) were plotted. Note that the more negative the relative error reduction value is, the closer the analysis is to the sonde. Overall, the RED_{137} experiment reduces the analysis error of temperature compared to the RED_{122} experiment over the entire atmospheric profile, especially in the troposphere. Figure 14.b shows that the addition of the 15 selected channels improves moisture analysis, especially in the lower troposphere, between 750 and 600 hPa and between 450

30   to 150 hPa compared to the RED_{122} experiment. On the contrary, there was a slight deterioration in the humidity analyses of the RED_{137} experiment compared to RED_{122} around 850 to 550 hPa. Finally, as expected, Figure 14.c shows that the RED_{137} experiment significantly improves ozone analysis compared to the RED_{122} experiment over a very large part of the atmosphere except in the lower troposphere. This near-surface degradation can be explained by the lack of sensitivity of the ozone-sensitive channels in the lower troposphere. Thus, for all the case studies representing different surfaces, latitudes and
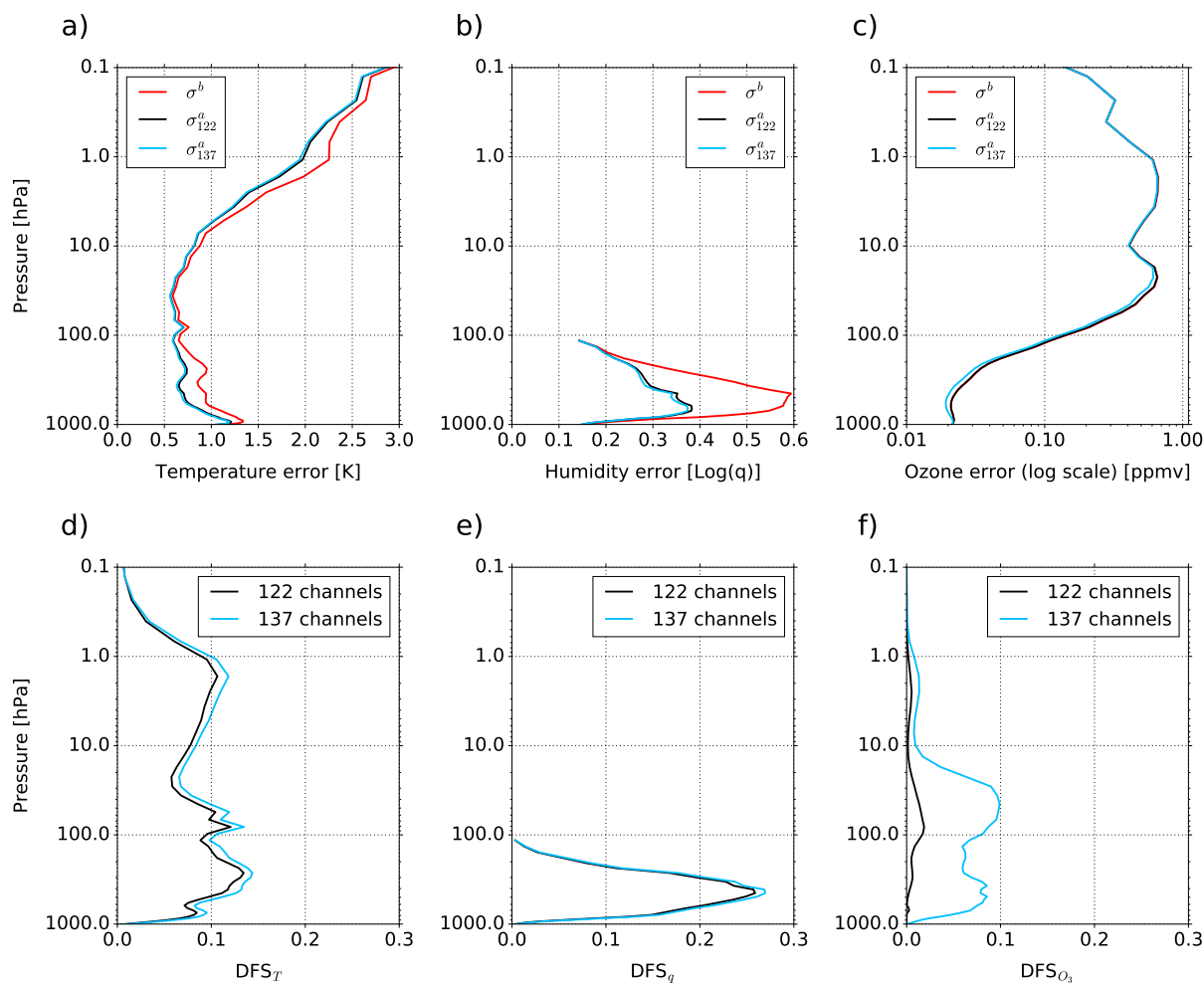
Figure 13. Vertical profiles of standard deviation of background errors (red line), analysis errors from 1D-Var experiments using 122 channels (black line) and using 137 channels (blue line) for temperature (a), humidity (b) and ozone (c). Vertical profiles of mean DFS over 345 profiles from 1D-Var experiments using 122 channels (black line) and using 137 channels (blue line) for temperature (d), humidity (e) and ozone (f).

seasons, the addition of this 15 ozone sensitive IASI channel selection improves temperature and humidity analyses and offers the possibility of improving ozone analyses in the case of data assimilation systems where the O_3 mixing ration is part of the control variable.

5   Summary and conclusions

5   This study has highlighted the potential of the information content provided by the IASI instrument on the atmosphere and particularly in the ozone-sensitive spectral band around 9.3 μm. Indeed, channels available in this spectral band are not only
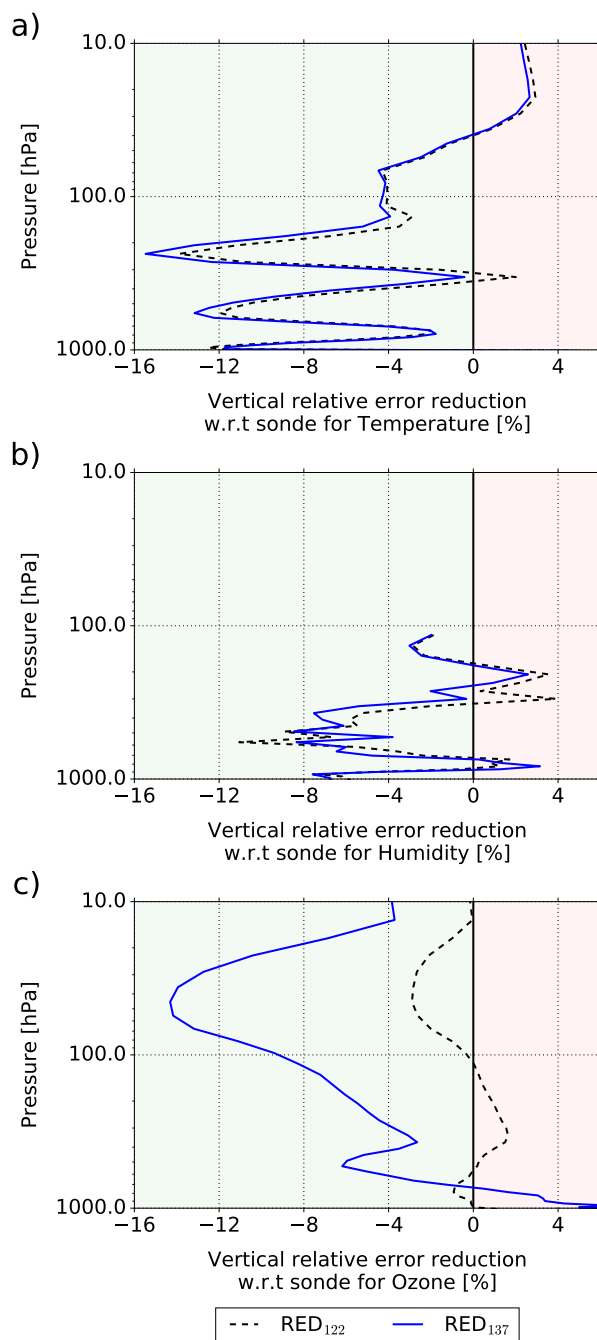
Figure 14. Vertical relative error reduction w.r.t sonde for 1D-Var experiment using 122 operational channels at Météo-France (black dashed line) and using 137 channels (122 operational + 15 O_3 selected channels) (blue line) for temperature (a), humidity (b) and ozone (c).

sensitive to ozone but also to temperature and water vapour. However, these channels are not used in the global NWP model ARPEGE at Météo-France. The increase in computing power allows us to use more radiances from IASI. A selection of 15 ozone sensitive IASI channels was performed by (Collard, 2007), but only to improve the ozone variable; a diagonal observation error covariance matrix **R** was used in his study. Nowadays, NWP centres are increasingly using full, diagnosed **R**

5   matrices to take into account the cross correlation errors between channels. Thus, the objective of this study was to perform a new selection of ozone-sensitive IASI channels from the full spectrum using a non diagonal **R** matrix on a set of 345 profiles representative of contrasted surface types, latitudes and seasons to also improve temperature and humidity analyses profiles.

In order to identify all ozone-sensitive channels over the entire spectrum, a physical method based on the non linear sen-

10   sitivity was done and 306 channels were pre-selected. Jacobians of these channels show that they are sensitive to ozone, to temperature in the troposphere and stratospheric environment, to humidity in the troposphere and to skin temperature. To determine the most informative ozone channels in terms of temperature, humidity, ozone and skin temperature, the DFS method has been chosen. This approach requires the specification of a covariance matrix of observational errors **R**, background error covariance matrix **B** and Jacobians of these channels. The matrix $\widetilde{\mathbf{R}}$ was diagnosed using the Desroziers method to take into

15   account the cross correlations between 306 ozone channels and 122 operational channels at Météo-France. The matrix **B** was calculated using the NMC method over a one-year period from CTM MOCAGE and the NWP model ARPEGE forecasts. Finally, the Jacobians were calculated using the RTTOV Radiative Transfer Model.

The average DFS results over 345 profiles indicate that the 306 ozone sensitive IASI channels provide additional information

20   compared to to the 122 operational channels. For temperature, the DFS increases from 3.57 to 5.20, for humidity it increases from 2.54 to 3.18, for ozone from 0.05 to 3.86 and for skin temperature from 0.979 to 0.994. When these 306 channels are added to the 122 operational ones, the information is mainly redundant in this part of the spectrum since only 39 channels provide 50 % of the available DFS with all 306 ozone channels. In order to select ozone channels that would most improve temperature and humidity analyses, several 1D-Var experiments have been carried out in a one-dimensional framework (1D-

25   Var). To quantify the contribution of ozone channels on analyses, we estimated the error reduction of the temperature, humidity and ozone analyses compared to their background using independent *in situ* sonde data as verification data. The results show that adding more ozone channels is not beneficial to the analysis. The non-linearity of the relative error reduction (RED) results as ozone-sensitive channels are added may be explained by the overall uncertainties in the use of 1D-Var. Moreover, the *a priori* profiles are already of good quality, which means that the threshold for improvement is limited. Finally, the sondes profiles do

30   not represent reality and can also have errors, which may explain why the analyses are less close to the verification data each time new channels are added. We also performed an 1D-Var experiment with the 15 channels selected by Collard whose results have been compared to the experiments with the different selections. The purpose of this selection is to provide information that can improve both temperature and humidity analysis and the best compromise for this is achieved with an experiment assimilating also 15 IASI channels sensitive to additional ozone. This revised channel selection reduces the analysis error on

35   average compared to only 122 channels. The RED in temperature decreases by 0.58 percentage points, in humidity by 0.62

percentage points and in ozone by 4.46 percentage points, which means an improvement, respectively, in temperature analysis of 13.8 %, in humidity of 20.9 % and in ozone of 1000 % compared to the analysis of the experiment with only 122 channels.

5   The vertical profiles of relative error reduction show that the assimilation of 15 additional selected channels improves tropospheric temperature analysis. The vertical DFS profiles of these channels show a maximum in the troposphere and also in the middle stratosphere but the sondes do not have data at these levels to verify. Finally, as expected, this channel selection significantly improves ozone analysis by up to 14 % in the lower stratosphere. The degradation of RED to ozone in the lower troposphere can be explained by the lack of sensitivity of ozone-sensitive channels in this part of the atmosphere. The improvement in the quality analyses are obtained at levels where Jacobians in temperature, humidity and ozone of the 15 selected

10   channels are maximum.

These results are very encouraging and allow us to propose a new selection of IASI ozone-sensitive channels for the global model ARPEGE. This selection provides the possibility to improve thermodynamic variable in the 4D-Var data assimilation and this study will be the subject of a future article.

15   *Code availability.* Codes of the Radiative Transfer Model RTTOV and the uni-dimensional data assimilation system 1D-Var used is this study are all available on https://www.nwpsaf.eu/site/software/rttov/download/.

Data availability. Data of radiosondes are available through this website: http://www.woudc.org. IASI data are available from EUMETSAT or AERIS: https://www.aeris-data.fr/. Model data are available upon request.

Competing interests. The authors declare that they have no conflict of interest.

20   *Acknowledgements.* This research has been conducted within the framework of O. Coopmann's PhD thesis, which funded by CNES (Centre National d'Études Spatiales) and the Région Occitanie. The authors would like to acknowledge Jean-François MAHFOUF for his help in revising and increasing the quality of the manuscript.

References

Anderson, D. C., Nicely, J. M., Wolfe, G. M., Hanisco, T. F., Salawitch, R. J., Canty, T. P., Dickerson, R. R., Apel, E. C., Baidar, S., Bannan, T. J., et al.: Formaldehyde in the Tropical Western Pacific: Chemical Sources and Sinks, Convective Transport, and Representation in CAM-Chem and the CCMI Models, Journal of Geophysical Research: Atmospheres, 122, 2017.

5 August, T., Klaes, D., Schlüssel, P., Hultberg, T., Crapeau, M., Arriaga, A., O'Carroll, A., Coppens, D., Munro, R., and Calbet, X.: IASI on Metop-A: Operational Level 2 retrievals after five years in orbit, Journal of Quantitative Spectroscopy and Radiative Transfer, 113, 1340–1371, 2012.

Bechtold, P., Bazile, E., Guichard, F., Mascart, P., and Richard, E.: A mass-flux convection scheme for regional and global models, Quarterly Journal of the Royal Meteorological Society, 127, 869–886, 2001.

10 Berre, L.: Estimation of synoptic and mesoscale forecast error covariances in a limited-area model, Monthly weather review, 128, 644–667, 2000.

Borbas, E. E., Hulley, G., Feltz, M., Knuteson, R., and Hook, S.: The Combined ASTER MODIS Emissivity over Land (CAMEL) Part 1: Methodology and High Spectral Resolution Application, Remote Sensing, 10, 643, 2018.

Bormann, N., Geer, A. J., and Bauer, P.: Estimates of observation-error characteristics in clear and cloudy regions for microwave imager
15 radiances from numerical weather prediction, Quarterly Journal of the Royal Meteorological Society, 137, 2014–2023, 2011.

Boukachaba, N.: Apport des observations satellitaires hyperspectrales infrarouges IASI au-dessus des continents dans le modèle météorologique à échelle convective AROME, Ph.D. thesis, INP Toulouse, http://www.theses.fr/2017INPT0065, 2017.

Bousserez, N., Attié, J., Peuch, V., Michou, M., Pfister, G., Edwards, D., Emmons, L., Mari, C., Barret, B., Arnold, S., et al.: Evaluation of the MOCAGE chemistry transport model during the ICARTT/ITOP experiment, Journal of Geophysical Research: Atmospheres, 112,
20 2007.

Boylan, P., Wang, J., Cohn, S. A., Fetzer, E., Maddy, E. S., and Wong, S.: Validation of AIRS version 6 temperature profiles and surface-based inversions over Antarctica using Concordiasi dropsonde data, Journal of Geophysical Research: Atmospheres, 120, 992–1007, 2015.

Burkholder, J. B., Sander, S. P., Abbatt, J. P. D., Barker, J. R., Huie, R. E., Kolb, C. E., Kurylo, M. J., Orkin, V. L., Wilmouth, D. M., and Wine, P. H.: Chemical Kinetics and Photochemical Data for Use in Atmospheric Studies. Evaluation No. 18, JPL Publication 15-10, 2015.

25 Clerbaux, C., Boynard, A., Clarisse, L., George, M., Hadji-Lazaro, J., Herbin, H., Hurtmans, D., Pommier, M., Razavi, A., Turquety, S., et al.: Monitoring of atmospheric composition using the thermal infrared IASI/MetOp sounder, Atmospheric Chemistry and Physics, 9, 6041–6054, 2009.

Collard, A.: Selection of IASI channels for use in numerical weather prediction, Quarterly Journal of the Royal Meteorological Society, 133, 1977–1991, 2007.

30 Coopmann, O., Guidard, V., Fourrié, N., and Plu, M.: Assimilation of IASI ozone-sensitive channels in preparation for an enhanced coupling between Numerical Weather Prediction and Chemistry Transport Models, Journal of Geophysical Research: Atmospheres, 2018.

Courtier, P., Freydier, C., Geleyn, J.-F., Rabier, F., and Rochas, M.: The Arpege project at Meteo France, in: ECMWF Seminar on Numerical Methods in Atmospheric Models, 9-13 September 1991, vol. II, pp. 193–232, ECMWF, Shinfield Park, Reading, https://www.ecmwf.int/node/8798, 1991.

35 Delcloo, A., Hurtmans, D., Coheur, P.-F., and Clerbaux, C.: Validation of IASI ozone profiles, using balloon sounding data, in: 2011 EU-METSAT meteorological satellite conference, https://hal.archives-ouvertes.fr/hal-00736646/document, 2011.

Derber, J. C. and Wu, W.-S.: The use of TOVS cloud-cleared radiances in the NCEP SSI analysis system, Monthly Weather Review, 126, 2287–2299, 1998.

Desroziers, G., Berre, L., Chapnik, B., and Poli, P.: Diagnosis of observation, background and analysis-error statistics in observation space, Quarterly Journal of the Royal Meteorological Society, 131, 3385–3396, 2005.

5   Dethof, A. and Holm, E.: Ozone assimilation in the ERA-40 reanalysis project, Quarterly Journal of the Royal Meteorological Society, 130, 2851–2872, 2004.

Dragani, R. and McNally, A.: Operational assimilation of ozone-sensitive infrared radiances at ECMWF, Quarterly Journal of the Royal Meteorological Society, 139, 2068–2080, 2013.

Fourrié, N. and Thépaut, J.-n.: Evaluation of the AIRS near-real-time channel selection for application to numerical weather prediction, Quarterly Journal of the Royal Meteorological Society, 129, 2425–2439, 2003.

10 Gambacorta, A. and Barnet, C. D.: Methodology and information content of the NOAA NESDIS operational channel selection for the Cross-Track Infrared Sounder (CrIS), IEEE Transactions on Geoscience and Remote Sensing, 51, 3207–3216, 2013.

Giorgi, F. and Chameides, W. L.: Rainout lifetimes of highly soluble aerosols and gases as inferred from simulations with a general circulation model, Journal of Geophysical Research: Atmospheres, 91, 14 367–14 376, 1986.

15 Guth, J., Josse, B., Marécal, V., Joly, M., and Hamer, P.: First implementation of secondary inorganic aerosols in the MOCAGE version R2.15.0 chemistry transport model, Geoscientific Model Development, 9, 137–160, https://doi.org/10.5194/gmd-9-137-2016, https://www.geosci-model-dev.net/9/137/2016/, 2016.

Guth, J., Marécal, V., Josse, B., Arteta, J., and Hamer, P.: Primary aerosol and secondary inorganic aerosol budget over the Mediterranean Basin during 2012 and 2013, Atmospheric Chemistry and Physics, 18, 4911–4934, https://doi.org/10.5194/acp-18-4911-2018, https://www.atmos-chem-phys.net/18/4911/2018/, 2018.

20 Han, W. and McNally, A.: The 4D-Var assimilation of ozone-sensitive infrared radiances measured by IASI, Quarterly Journal of the Royal Meteorological Society. Meteor. Soc., 136, 2025–2037, 2010.

Hilton, F., Armante, R., August, T., Barnet, C., Bouchard, A., Camy-Peyret, C., Capelle, V., Clarisse, L., Clerbaux, C., Coheur, P.-F., et al.: Hyperspectral Earth observation from IASI: Five years of accomplishments, Bulletin of the American Meteorological Society, 93, 347–370, 2012.

25 Hólm, E. V. and Kral, T.: Flow-dependent, geographically varying background error covariances for 1D-VAR applications in MTG-IRS L2 Processing, ECMWF Technical Memoranda, p. 15, https://doi.org/10.21957/3yx4fe6cv, https://www.ecmwf.int/node/9997, 2012.

Ide, K., Courtier, P., Ghil, M., and Lorenc, A. C.: Unified Notation for Data Assimilation: Operational, Sequential and Variational (gtSpecial IssueltData Assimilation in Meteology and Oceanography: Theory and Practice), Journal of the Meteorological Society of Japan. Ser. II, 30   75, 181–189, 1997.

Josse, B., Simon, P., and Peuch, V.-H.: Radon global simulations with the multiscale chemistry and transport model MOCAGE, Tellus B: Chemical and Physical Meteorology, 56, 339–356, 2004.

Lefevre, F., Brasseur, G., Folkins, I., Smith, A., and Simon, P.: Chemistry of the 1991–1992 stratospheric winter: Three-dimensional model simulations, Journal of Geophysical Research: Atmospheres, 99, 8183–8195, 1994.

35 Lefèvre, F., Figarol, F., Carslaw, K. S., and Peter, T.: The 1997 Arctic ozone depletion quantified from three-dimensional model simulations, Geophysical research letters, 25, 2425–2428, 1998.

Louis, J.-F.: A parametric model of vertical eddy fluxes in the atmosphere, Boundary-Layer Meteorology, 17, 187–202, 1979.

Lupu, C. and McNally, A.: Wind tracing with ozone-sensitive radiances from SEVIRI, p. 22, https://www.ecmwf.int/node/10862, 2013.

Madronich, S.: Photodissociation in the atmosphere: 1. Actinic flux and the effects of ground reflections and clouds, Journal of Geophysical Research: Atmospheres, 92, 9740–9752, 1987.

Marécal, V., Peuch, V.-H., Andersson, C., Andersson, S., Arteta, J., Beekmann, M., Benedictow, A., Bergström, R., Bessagnet, B., Cansado, A., et al.: A regional air quality forecasting system over Europe: the MACC-II daily ensemble production, 2015.

5 Mari, C., Jacob, D. J., and Bechtold, P.: Transport and scavenging of soluble gases in a deep convective cloud, Journal of Geophysical Research: Atmospheres, 105, 22 255–22 267, 2000.

Morgenstern, O., Hegglin, M., Rozanov, E., O'Connor, F. M., Abraham, N. L., Akiyoshi, H., Archibald, A., Bekki, S., Butchart, N., Chipperfield, M. P., et al.: Review of the global models used within phase 1 of the Chemistry-Climate Model Initiative (CCMI), Geoscientific Model Development, 10, 639–671, 2017.

10 Parrish, D. F. and Derber, J. C.: The National Meteorological Center's spectral statistical-interpolation analysis system, Monthly Weather Review, 120, 1747–1763, 1992.

Rodgers, C. D.: Inverse methods for atmospheric sounding: theory and practice, vol. 2, World scientific, 2000.

Rodgers, C. D. and Connor, B. J.: Intercomparison of remote sounding instruments, Journal of Geophysical Research: Atmospheres, 108, 2003.

15 Saunders, R. W. and Kriebel, K. T.: An improved method for detecting clear sky and cloudy radiances from AVHRR data, International Journal of Remote Sensing, 9, 123–150, 1988.

Semane, N., Peuch, V.-H., Pradier, S., Desroziers, G., Amraoui, L. E., Brousseau, P., Massart, S., Chapnik, B., and Peuch, A.: On the extraction of wind information from the assimilation of ozone profiles in Météo–France 4-D-Var operational NWP suite, Atmospheric Chemistry and Physics, 9, 4855–4867, 2009.

20 Sherlock, V. and Saunders, R.: ISEM-6: Infrared surface emissivity model for RTTOV-6, NWP-SAF report, https://www.nwpsaf.eu/site/download/documentation/rtm/papers/isem6.pdf, 1999.

Stockwell, W. R., Kirchner, F., Kuhn, M., and Seefeld, S.: A new mechanism for regional atmospheric chemistry modeling, Journal of Geophysical Research: Atmospheres, 102, 25 847–25 879, 1997.

Ventress, L. and Dudhia, A.: Improving the selection of IASI channels for use in numerical weather prediction, Quarterly Journal of the Royal Meteorological Society, 140, 2111–2118, 2014.

25 Vincensini, A.: Contribution de IASI à l'estimation des paramètres des surfaces continentales pour la prévision numérique du temps, Ph.D. thesis, École Doctorale Sciences de l'univers, de l'environnement et de l'espace, 2013.

Wesely, M.: Parameterization of surface resistances to gaseous dry deposition in regional-scale numerical models, Atmospheric Environment, 41, 52–63, 2007.

30 Weston, P., Bell, W., and Eyre, J.: Accounting for correlated error in the assimilation of high-resolution sounder data, Quarterly Journal of the Royal Meteorological Society, 140, 2420–2429, 2014.

Williamson, D. L. and Rasch, P. J.: Two-dimensional semi-Lagrangian transport with shape-preserving interpolation, Monthly Weather Review, 117, 102–129, 1989.